NASA MEMO 10-8-58A

NASA

MEMORANDUM

AN INVESTIGATION OF THE DRAG CHARACTERISTICS OF A TAILLESS DELTA-WING AIRPLANE IN FLIGHT, INCLUDING COMPARISON WITH WIND-TUNNEL DATA

By L. Stewart Rolls and Rodney C. Wingrove

Ames Research Center
Moffett Field, Calif.

NATIONAL AERONAUTICS AND SPACE ADMINISTRATION

WASHINGTON

November 1958

Declassified July 11, 1961

CONFIDENTIAL

NATIONAL AERONAUTICS AND SPACE ADMINISTRATION

MEMORANDUM 10-8-58A

AN INVESTIGATION OF THE DRAG CHARACTERISTICS OF A TAILLESS DELTA-WING AIRPLANE IN FLIGHT, INCLUDING COMPARISON WITH WIND-TUNNEL DATA

By L. Stewart Rolls and Rodney C. Wingrove

SUMMARY

A series of flight tests were conducted to determine the lift and drag characteristics of an F4D-1 airplane over a Mach number range of 0.80 to 1.10 at an altitude of 40,000 feet. Apparently satisfactory agreement was obtained between the flight data and results from wind-tunnel tests of an 0.055-scale model of the airplane. Further tests show the apparent agreement was a consequence of the altitude at which the first tests were made.

INTRODUCTION

Lately several prototype aircraft have exhibited severe performance discrepancies when their actual performance capabilities were compared with their estimated capabilities based on wind-tunnel tests. These performance discrepancies could result from either an erroneous determination of airplane drag in the wind tunnel or an inaccurate prediction of the thrust available from the propulsion system.

Previously it has been difficult to obtain accurate drag measurements in flight. New techniques in instrumentation, such as more sensitive longitudinal accelerometers, and more precise determination of angle of attack have enabled the accurate determination in flight by the accelerometer method (ref. 1) of the drag due to lift.

During a flight-test investigation of a tailless delta-wing airplane, drag measurements were made over the Mach number range of 0.70 to 1.10 at 40,000 feet and of 0.7 to 0.89 at 8,000 feet altitude. In addition to the constant altitude data the effect of Reynolds number was investigated by making measurements at Mach numbers 0.8 and 1.05 over the altitude capability range of the airplane. The results of this investigation reported herein are compared with unpublished 0.055-scale model data from the Ames 14-foot transonic wind tunnel.

NOTATION

A	aspect ratio
A_l	measured longitudinal acceleration, g's
A_n	measured normal acceleration, g's
A_x	true airplane longitudinal acceleration, g's
A_z	true airplane normal acceleration, g's
C_D	drag coefficient, $\frac{\text{drag}}{q_\infty S}$
C_{D_i}	induced drag coefficient, $C_{D_T} - C_{D_O}$
C_{D_T}	total measured drag coefficient
C_{D_O}	drag coefficient at zero lift
C_f	nozzle coefficient
C_L	lift coefficient, $\frac{\text{lift}}{q_\infty S}$
C_{L_α}	lift-curve slope
C_N	normal-force coefficient, $\frac{WA_n}{q_\infty S}$
D_x	drag force along airplane axis, lb
F_G	jet engine gross thrust, lb
h_p	pressure altitude
L_N	lift force normal to airplane axis, lb
M	Mach number
M.A.C.	mean aerodynamic chord

P	total pressure in tail pipe, lb/ft^2
p_∞	free-stream static pressure, lb/ft^2
q_∞	free-stream dynamic pressure, lb/ft^2
R	Reynolds number
S	wing area, ft^2
V_∞	free-stream velocity, ft/sec
W	weight, lb
w_a	air flow through jet engine, slugs/sec
α	angle of attack, deg
γ	flight-path angle, deg
δ_e	elevon deflection, deg
δ_{PT}	pitch-trimmer deflection, deg
ΔC	correction to lift and drag coefficients due to elevon deflection

EQUIPMENT AND TESTS

Airplane

The airplane used during this investigation was an F4D-1 - a tailless, modified delta-wing, single-place fighter. The pertinent dimensions are presented in table I. A photograph and a diagrammatic sketch of the test airplane are shown in figures 1 and 2, respectively. The test airplane was powered with a J57-P-8A turbojet engine with a rated thrust of 10,200 pounds in military power and 16,000 pounds in afterburning. The airplane is equipped with a set of elevons for longitudinal and lateral control and a set of trimmers mounted at the inboard trailing edge of the wing for trimming the aircraft.

Instruments and Methods

NACA photographic recording instruments and a recording oscillograph were used to record the test data. They were synchronized at 1/10-second intervals by a single timer circuit. True Mach numbers were calculated

from measurements of total and static pressures obtained with a 10-foot nose boom. A calibration of this airspeed installation was obtained by the "fly-by" method up to a Mach number of 0.98. This calibration was extrapolated to higher Mach numbers by use of data obtained during the passage of a fuselage bow wave over the static orifices on the airspeed head at high Mach numbers (see ref. 2).

The equations used to compute the airplane lift and drag from measurements of the normal and longitudinal acceleration, engine thrust, and angle of attack are presented in the appendix.

To measure the angle of attack, a vane was mounted on the nose boom 6.8 feet in front of the airplane. The methods outlined in reference 3 were used to investigate the necessary corrections to the measured angle of attack. To determine the upwash at the vane station a five-vane angle-of-attack boom (fig. 3) similar to that of reference 3 was mounted on the airplane. The variation of local angle of attack with distance in front of the airplane is shown in figure 4. The regular vane corresponds to the location of vane 4 on this boom. As shown in figure 4 the upwash at vane 4 is negligible and hence it was not necessary to correct the data measured at the regular vane station for upwash. Data from additional runs indicate that the upwash is also small at higher Mach numbers. The upwash around the boom was also sufficiently small to be neglected. The major corrections applied to the angle-of-attack data were those due to boom bending and vane floating angle.

The computations of engine thrust and air flow are based upon measurements of the jet exhaust pressure and temperature and employed the method of reference 4. The total pressure of the jet exhaust is measured with an air-cooled, fixed, total-pressure probe similar to the one shown in reference 5. The jet-exhaust temperature was taken from a reading of the tail-pipe exhaust temperature indicator. The thrust-measuring system was calibrated on a ground thrust stand and in flight. The flight portion of the calibration was based on flights wherein the drag force was held approximately constant by taking data at the same Mach number and pressure altitude in zero g flight but with different levels of thrust, that is, at various flight path angles. The drag was assumed to be fixed and the effect of the changing engine pressure ratio on the base and boattail drag was assumed to be negligible. It was then possible to derive the variation of nozzle coefficient with engine pressure ratio. The nozzle coefficient as determined on the thrust stand and in flight is presented in figure 5. The difference in the level of the curves for afterburner on and off is believed to be caused by the change in location of the probe with respect to the tail pipe when the afterburner eyelids are opened. Since net-thrust coefficient is constant at the higher pressure ratios, a value of 0.915 was used for nonafterburner runs and a value of 0.955 was used for afterburner runs above a pressure ratio of 3.6. This method of thrust measurement includes the losses in the jet-exhaust ejector as airplane drag. The "swinging probe" or jet

exhaust survey technique described in references 5 and 6 can be used to separate these ejector losses from the airplane drag; however, this refinement was not considered necessary in this present study as the dimensions of the fuselage exit (diameter ratio 2.0, spacing ratio 0) are such that one would expect little ejector action for the test airplane.

The wind-tunnel data for correlation were obtained primarily from tests of an 0.055-scale model in the Ames 14-foot transonic wind tunnel. The full-span model was sting mounted and the data have been corrected for wind-tunnel stream angularity. The model simulates the correct full-scale configuration with the exception that the model did not include the nose boom or the slots and gaps in the wing associated with the leading-edge slots.

In order to estimate the precision of the drag data, the uncertainty in each of the measured quantities was converted into the following errors in drag coefficient (based on a dynamic pressure of 250 pounds per square foot and conditions at 40,000 feet altitude).

Thrust (normal rated)	±0.0006
Angle of attack	±0.0004
Normal acceleration	±0.0002
Longitudinal acceleration	±0.0006
Dynamic pressure	±0.0008

A standard deviation of the uncertainties was computed using the method presented in reference 3. These results indicate the error in drag coefficient should be less than 0.0007 fifty-eight percent of the time. The accuracy in measured Mach number is ±0.01 except in the range of 0.95 to 1.02 where the Mach number error is ±0.02.

Tests

The test maneuver used to obtain the data was a gradual push-down from level, trimmed flight to approximately zero g's, followed by a gradual pull-up to limit load factor or the buffet boundary, whichever occurred first. The time required for the maneuver from zero g's to limit load factor was from 20 to 25 seconds. The data were analyzed for constant intervals of time beginning at the point of minimum normal acceleration. Prior to the run the engine thrust was adjusted to that required for level flight and remained nearly constant during the run. At high speeds the use of the afterburner and a slight dive angle were required to obtain the desired Mach number.

The variation of Reynolds number with Mach number in flight at 40,000 and 8,000 feet and for the wind-tunnel tests is presented in figure 6.

RESULTS AND DISCUSSION

Basic Data

Typical curves showing the flight-measured lift and drag characteristics at a pressure altitude of 38,000 to 41,000 feet are presented in figure 7. During some of the maneuvers some variation in Mach number occurred; hence, the variation of Mach number with lift coefficient is also shown in this figure. The data in these figures indicate smooth curves with a scatter consistent with the previously computed probable error of 0.0007. The data are for the airplane trimmed for the particular Mach number, including the drag due to the elevon and trimmer deflections required to get the desired normal acceleration factor. Similar lift and drag polars for the test airplane in trimmed flight at 8,000 feet altitude are shown in figure 8.

With the use of the data presented in figure 7 and additional data at other Mach numbers, the variation of airplane drag with Mach number at constant lift coefficient was plotted. These results are presented in figure 9, where the variation of airplane drag coefficient with Mach number is presented for values of lift coefficient of 0, 0.2, 0.25, 0.3, and 0.4.

Correlation With Wind-Tunnel Tests

A series of tests of a model of the F4D-1 airplane were conducted in the Ames 14-foot transonic wind tunnel for the purposes of studying the drag of the basic aircraft and the effect of stores. The results of these investigations afford an opportunity to correlate the wind-tunnel drag characteristics with the flight-measured characteristics.

The model tests were conducted with a 0.05-scale model of the F4D at very low Reynolds numbers compared with flight as shown in figure 6. The model used in this investigation was as close to a correct representation of the full-scale aircraft as was possible; however, the model did not contain the slots and gaps associated with the closed leading-edge slat and the control surfaces were fixed at zero deflection. While some internal flow through the side inlets was present, the flow quantity did not exactly represent that encountered in flight and the drag difference due to this mass-flow discrepancy was estimated to be about -0.0010. The model surface was smooth and fair and no attempt was made to fix the boundary-layer transition point on the model. The model data have been corrected for base pressure effects of the sting support by measuring base pressure and adjusting the drag to correspond to free-stream static pressure acting on the base area.

In order to correlate the flight data with the wind-tunnel data it is necessary to take account of the elevon and trimmer deflections which occur during flight. The corrections to the lift and drag are based on the data from the Ames 6- by 6-foot supersonic wind tunnel that are presented in reference 7. Since there were two series of flight data in this report with different variations of elevon angles with lift coefficient, it was decided to correct the flight data to zero elevon deflection to correspond to the wind-tunnel data. The curves shown in figure 10 illustrate the magnitude of the corrections which were applied to the flight data to obtain lift and drag polars for zero elevon angle. During the majority of the test maneuvers the pitch-trimmer deflection was small ($\delta_{PT} \approx 3^\circ$), and consequently the drag correction for the pitch-trimmer deflection was negligible. In the "trim change" Mach number region (M = 0.96 to 0.98) a trimmer angle of about 11° was required which resulted in a drag increment due to correcting for the trimmer deflection of about -0.0060. For the wind-tunnel data, a constant increment of drag of -0.0010 was added to account for the aforementioned internal flow losses.

A series of drag polars showing the correlation between flight and wind-tunnel data is shown in figure 11. The data in figure 11 show surprisingly good correlation between flight and wind-tunnel tests except for the higher lift coefficients in the range of Mach numbers corresponding to the drag rise (M = 0.90 to 1.00). In this range of Mach numbers the comparison is the least accurate due to the increased uncertainty in the Mach number and in the corrections applied for the in-flight elevon deflections. This Mach number range is also in the trim-change region and where the reduced elevon effectiveness requires the use of large elevon deflections. These wind-tunnel and flight data are for vastly different Reynolds numbers and would not be expected to be in agreement. Further tests made to investigate Reynolds number effects will be discussed in subsequent sections.

Drag Due to Lift

The variation of the drag-rise factor with Mach number as measured in flight at altitudes of 8,000 and 40,000 feet and in the wind tunnel are presented in figure 12(a). The data used to compute the drag-rise factor ($\partial C_D/\partial C_L^2$) were corrected for the effect of elevon and pitch-trimmer deflections. Also shown in this figure, for comparison, are the drag-rise factors computed with the assumption of (1) an elliptic spanwise distribution of lift with full leading-edge suction at subsonic speeds ($\partial C_D/\partial C_L^2 = 1/\pi A$), and (2) no leading-edge suction so that the resultant force vector due to angle of attack is perpendicular to the wing chord ($\partial C_D/\partial C_L^2 = 1/57.3\ C_{L_\alpha}$). The flight-determined lift-curve slope at an altitude of 40,000 feet, used to compute the values of $1/57.3\ C_{L_\alpha}$, are presented in figure 12(b). Comparison of the drag-rise

factor at 40,000 and at 8,000 feet indicates that in the range of these tests the drag-rise factor is lower for the higher Reynolds numbers (lower altitude). A similar conclusion cannot be derived from the comparison with wind-tunnel data except at Mach numbers of 0.80 to 0.89. Differences between flight and wind-tunnel data may result from the differences in Reynolds number or aeroelastic effects. Calculations have indicated the aeroelastic effects in flight are negligible.

Reynolds Number Effects

On minimum drag coefficient.- The effect of Reynolds number on the zero lift drag was investigated by obtaining data during zero g flight over a wide altitude range at Mach numbers of 0.80 and 1.05. The altitude range was 5,000 to 54,000 feet at a Mach number of 0.80. The variation of drag coefficient at zero lift with Reynolds number is shown in figure 13. Between the time the data on this figure and the data presented elsewhere in the report were obtained the airplane was structurally modified. These modifications changed the aft fuselage lines and the base area which resulted in an increase of approximately 0.0035 in minimum drag coefficient. The variation of skin-friction drag with Reynolds number, assuming the whole aircraft surface area of 1,500 square feet to be in either a turbulent or laminar condition, is presented in figure 13 for comparison. The laminar or turbulent skin-friction coefficients were obtained from the equations in reference 8 for flat plates at $M = 0.8$. The flight data for a Mach number of 0.80 indicate that as the Reynolds number is decreased below 30 million the zero lift drag decreases to about 5/6 of its higher Reynolds number value. The same trend is indicated at a Mach number of 1.05, however, as low a Reynolds number was not obtained. Also shown in figure 13, at their appropriate Reynolds numbers, are the results from model tests in several wind tunnels (refs. 7 and 9). These data are for the unmodified configuration and as stated previously would be 35 counts of drag less than the flight data. The level of the model data indicates that during the wind-tunnel tests the flow was primarily turbulent.

To investigate the precision of the drag measurements at the lower flight Reynolds numbers the drag coefficients were measured at different amounts of thrust at a constant pressure altitude of 45,000 feet. This way the two quantities (F_G and WA_X) in the equation for determining drag (see appendix) were drastically changed and the uncertainty in drag determination minimized. The effect of changing engine power on the zero lift drag is shown in figure 14. It will be noted that the changes in thrust had no effect on the measured drag level. The data at the lowest pressure ratio indicated a difference of 0.0008 in drag coefficient which is within the stated accuracy of the data. Thus the trends indicated in figure 13 at the low Reynolds numbers are not the result of changes in engine power (pressure ratio).

On the drag due to lift.- A series of push-down, pull-up maneuvers were performed over the altitude range at Mach numbers of 1.05 and 0.80 to evaluate the effect of Reynolds number on the drag due to lift. The variation of the drag-rise factor ($\delta C_D/\delta C_L^2$) with Reynolds number is presented in figure 15. These data are based on the slope of the C_D versus C_L^2 curves for the C_L range of 0.05 to 0.15. These data are for the airplane in trimmed flight and have not been adjusted for the elevon angle or trimmer deflection used during the maneuvers. The data for the Mach number of 0.80 exhibited a discontinuity in the C_D versus C_L^2 curve as shown in figure 16 for Reynolds number below about 30 million. The slope of the C_D versus C_L^2 curve below the break was used for the curve of $\delta C_D/\delta C_L^2$ versus Reynolds number shown in figure 15. If the slope of the curve above the break were used, the drag-rise factor would decrease continuously from Reynolds numbers of 17 to 80 million. A break in the C_D versus C_L^2 curves may exist at a Mach number of 1.05 but because of the inability to get data over a wide enough lift coefficient and Reynolds number range it was not possible to evaluate the complete trends at that Mach number.

Also indicated in figure 15 are the values of drag-rise factor with full leading-edge suction at subsonic speeds ($1/\pi A$) and no leading-edge suction ($1/57.3\ C_{L_\alpha}$). The value of drag-rise factor as measured in the Ames 14-foot transonic wind tunnel and the Ames 6- by 6-foot supersonic wind tunnel, for elevon and trimmers undeflected, is also shown for comparison.

CONCLUDING REMARKS

The agreement between the flight and tunnel data presented in figure 11 is misleading and results from the altitude selected for obtaining these flight data. The variation of C_{D_o} and $\delta C_D/\delta C_L^2$ as a function of Reynolds number as shown in figures 13 and 15 indicates a sizable change in these quantities with Reynolds number; thus the agreement in figure 11 for flight and wind-tunnel drag measurements is fortuitous. An extrapolation of the wind-tunnel data along a line parallel to the turbulent skin-friction drag curve to the flight Reynolds numbers indicates a much lower C_{D_o} at the flight Reynolds numbers than the flight measured C_{D_o} (fig. 13). This drag difference is probably the result of gaps, slots, grooves, bumps, and surface discontinuities occurring on the actual aircraft. The wind-tunnel model was smooth.

Ames Research Center
National Aeronautics and Space Administration
Moffett Field, Calif., May 9, 1957

APPENDIX

DETERMINATION OF LIFT AND DRAG

The evaluation of the lift and drag forces on the airframe as presented in this report was based on the application of the accelerometer method described in reference 1.

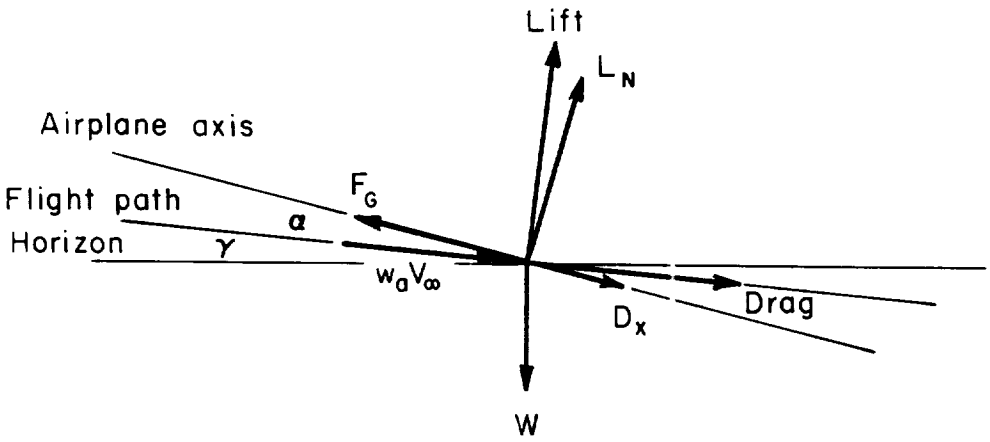

Summing the forces and accelerations along the airplane axis and equating them to zero yields

$$F_G - w_a V_\infty \cos \alpha - D_X - W \sin(\alpha + \gamma) - WA_X = 0 \qquad (A1)$$

However, the longitudinal accelerometer is affected by gravity,

$$A_X = A_l - \sin(\alpha + \gamma) \qquad (A2)$$

Combining equations (A1) and (A2) gives

$$F_G - w_a V_\infty \cos \alpha - D_X - W \sin(\alpha + \gamma) - W [A_l - \sin(\alpha + \gamma)] = 0$$

$$F_G - w_a V_\infty \cos \alpha - D_X - WA_l = 0$$

$$D_X = F_G - w_a V_\infty \cos \alpha - WA_l \qquad (A3)$$

Summing forces perpendicular to the airplane axis and equating to zero gives

$$W \cos(\alpha + \gamma) - L_N + WA_Z - w_a V_\alpha \sin \alpha = 0 \qquad (A4)$$

However, the normal accelerometer is also affected by gravity; hence

$$A_z = A_n - \cos(\alpha + \gamma) \tag{A5}$$

Combining equations (A4) and (A5) gives

$$W \cos(\alpha + \gamma) - L_N + W [A_n - \cos(\alpha + \gamma)] - w_a V_\infty \sin \alpha = 0$$

$$L_N = WA_n - w_a V_\infty \sin \alpha \tag{A6}$$

The force coefficients of equations (A3) and (A6) can be corrected from the airplane axis to the flight-path axis as follows

$$\text{Lift} = W(A_n \cos \alpha + A_l \sin \alpha) - F_G \sin \alpha \tag{A7}$$

$$\text{Drag} = W(A_n \sin \alpha - A_l \cos \alpha) + F_G \cos \alpha - w_a V_\infty \tag{A8}$$

The weight of the airplane was determined from the take-off weight and the amount of fuel used between the take-off and the time of the run.

REFERENCES

1. Keller, Thomas L., and Keuper, Robert F.: Comparison of the Energy Method with the Accelerometer Method of Computing Drag Coefficients from Flight Data. NACA WR A-57, 1945. (Supersedes NACA CB 5H31)

2. Thompson, Jim Rogers, Bray, Richard S., and Cooper, George E.: Flight Calibration of Four Airspeed Systems on a Swept-Wing Airplane at Mach Numbers up to 1.04 by the NACA Radar-Phototheodolite Method. NACA TN 3526, 1955.

3. McFadden, Norman M., Holden, George R., and Ratcliff, Jack W.: Instrumentation and Calibration Technique for Flight Calibration of Angle-of-Attack Systems on Aircraft. NACA RM A52I23, 1952.

4. Beeler, De Elroy, Bellman, Donald R., and Saltzman, Edwin J.: Flight Techniques for Determining Airplane Drag at High Mach Numbers. NACA TN 3821, 1956.

5. Rolls, L. Stewart, Havill, C. Dewey, and Holden, George R.: Techniques for Determining Thrust in Flight for Airplanes Equipped with Afterburners. NACA RM A52K12, 1953.

6. Havill, C. Dewey, and Rolls, L. Stewart: A Sonic-Flow Orifice Probe for the In-Flight Measurement of Temperature Profiles of a Jet Engine Exhaust With Afterburning. NACA TN 3714, 1956.

7. Drake, D. E.: Summary and Stability and Control Analysis of Transonic Wind-Tunnel Tests of the Model F4D-1 Airplane. Rep. No. E.S. 26179, Douglas Aircraft Co., Inc., Feb. 16, 1956.

8. Van Driest, E. R.: Turbulent Boundary Layer in Compressible Fluids. Jour. Aero. Sci., vol. 18, no. 3, March 1951, pp. 145-160.

9. Smith, Willard G.: Wind-Tunnel Investigation at Subsonic and Supersonic Speeds of a Model of a Tailless Fighter Airplane Employing a Low-Aspect-Ratio Swept-Back Wing - Effects of External Fuel Tanks and Rocket Packets on the Drag Characteristics. NACA RM A52J31, 1953.

TABLE I.- DIMENSIONAL DATA FOR THE F4D-1 AIRPLANE

Fuselage	
Length, ft	38.63
Fineness ratio	6.53
Wing	
Airfoil section	
Root	NACA 0007 (Mod.)
Tip	NACA 0004.5 (Mod.)
Span, ft	33.5
Area, sq ft	557.0
Taper ratio	0.332
Aspect ratio	2.02
Mean aerodynamic chord, ft	18.25
Elevon	
Area, sq ft (total)	45.14
Pitch trimmer	
Area, sq ft (total)	26.84
Vertical tail	
Area, sq ft	47.7
Span, ft	7.58
Rudder	
Area, sq ft	12.4

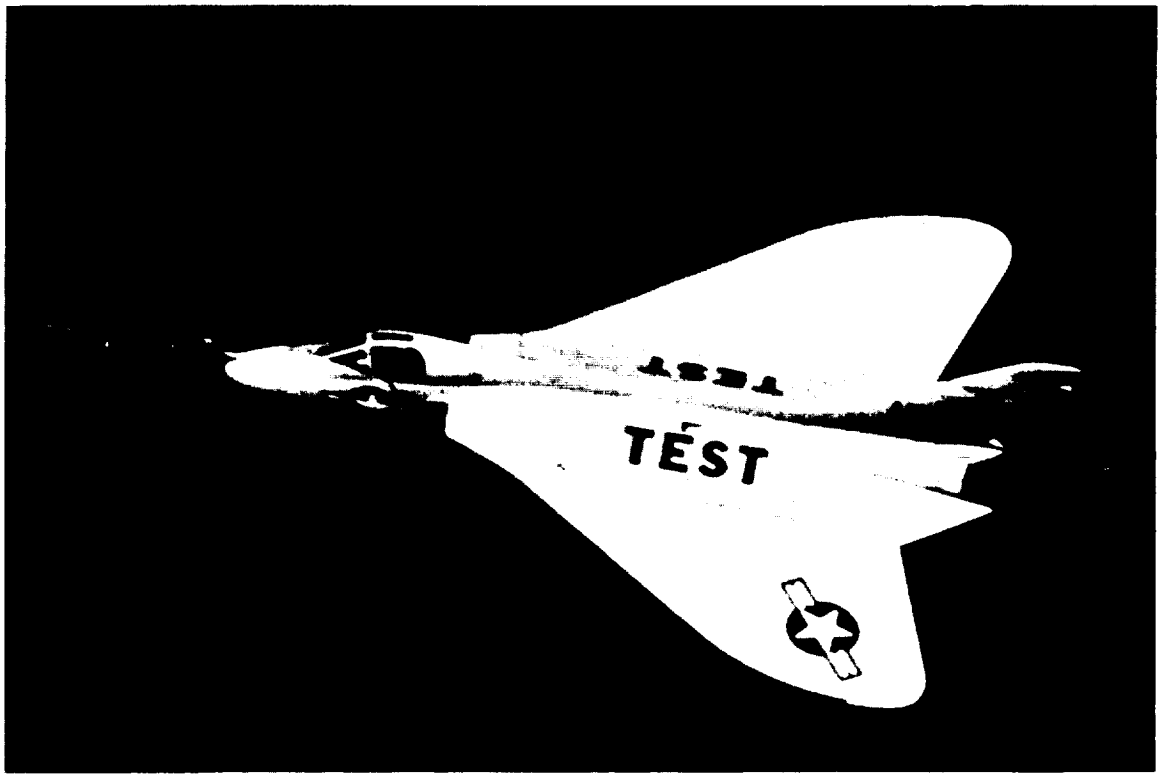

A-22215

Figure 1.- The test airplane.

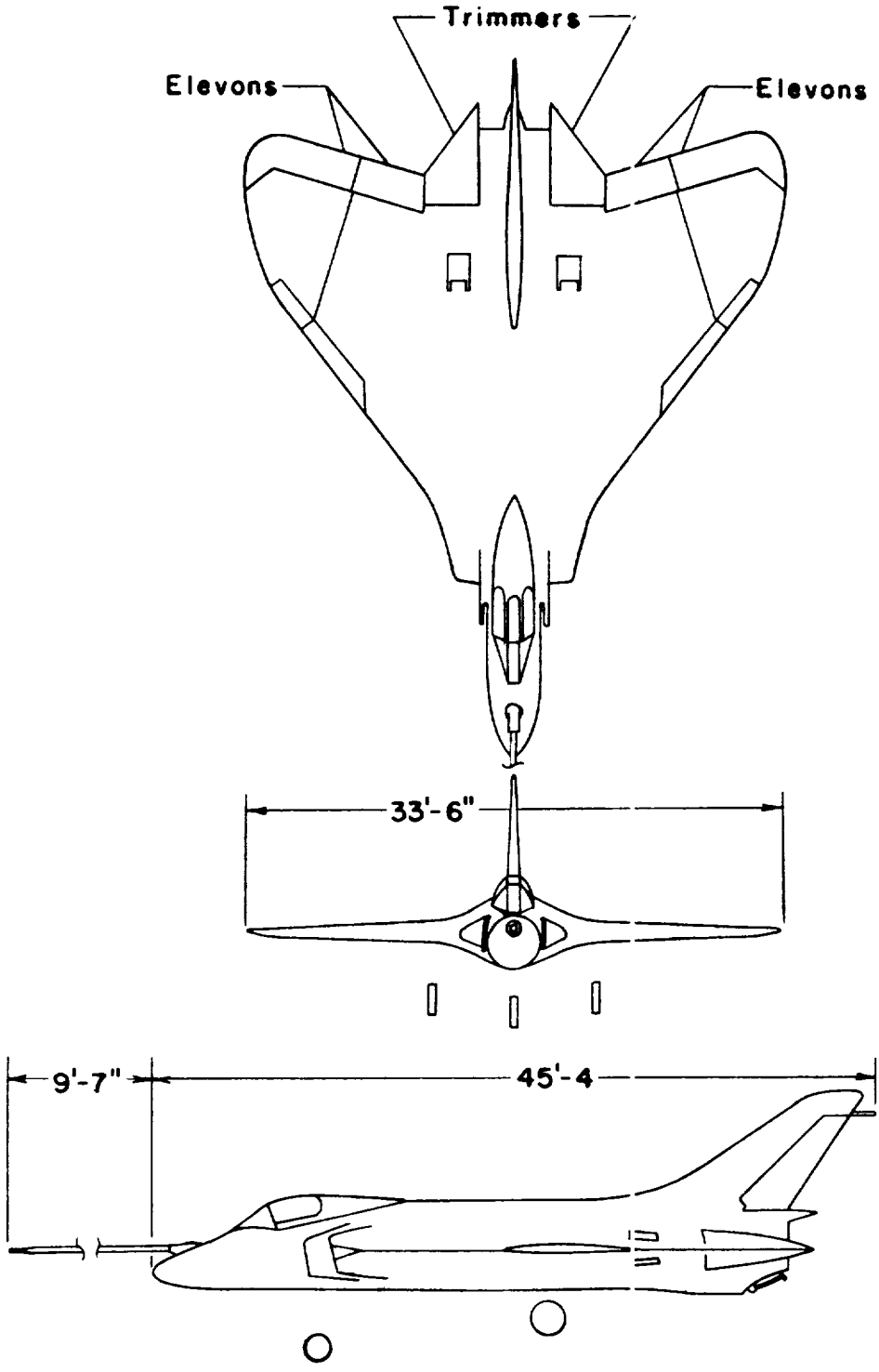

Figure 2.- Three-view drawing of test airplane.

A-22150

Figure 3.- Special boom used to measure upwash ahead of airplane to calibrate angle-of-attack vane.

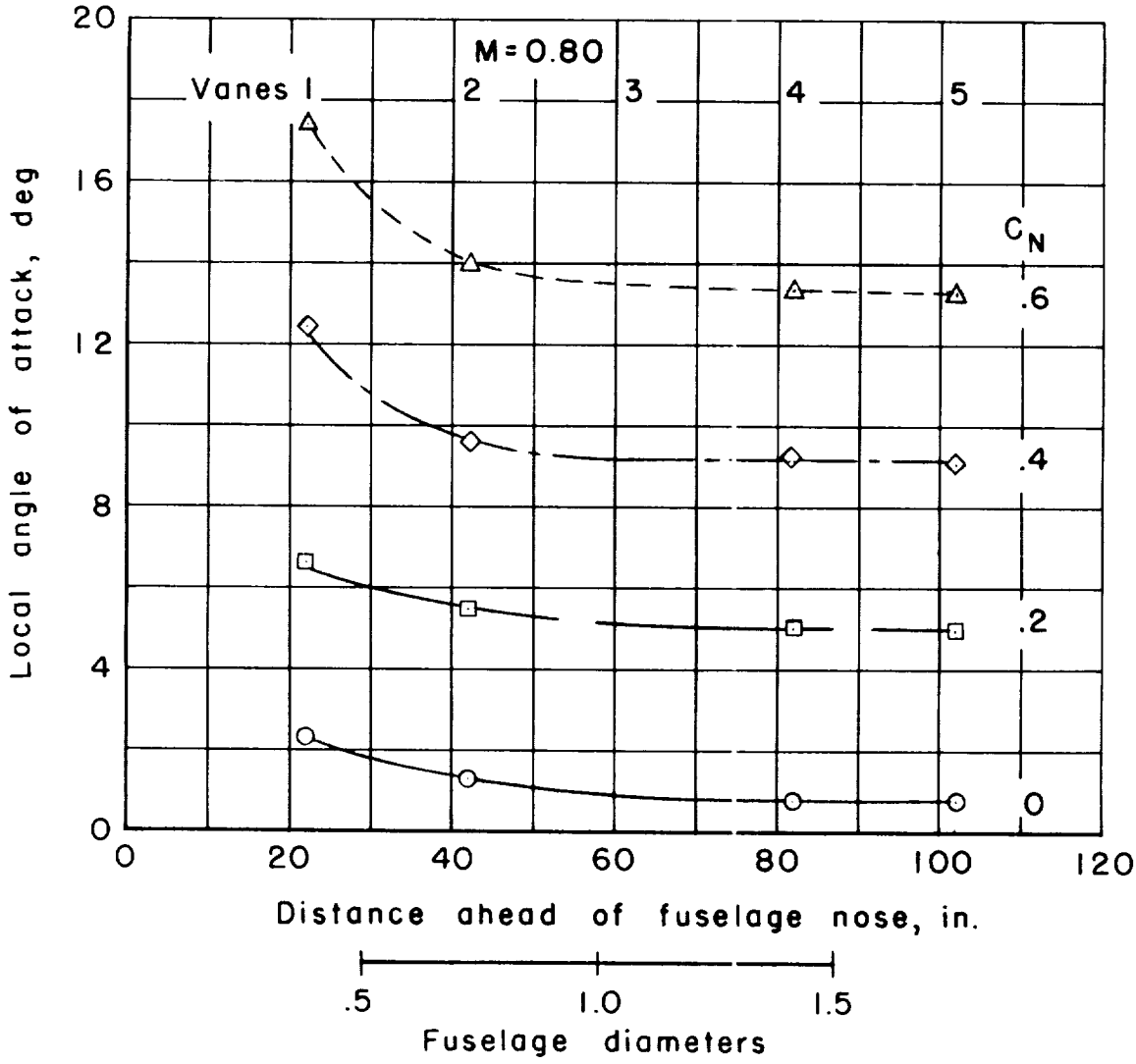

Figure 4.- Variation of local angle of attack with distance ahead of fuselage.

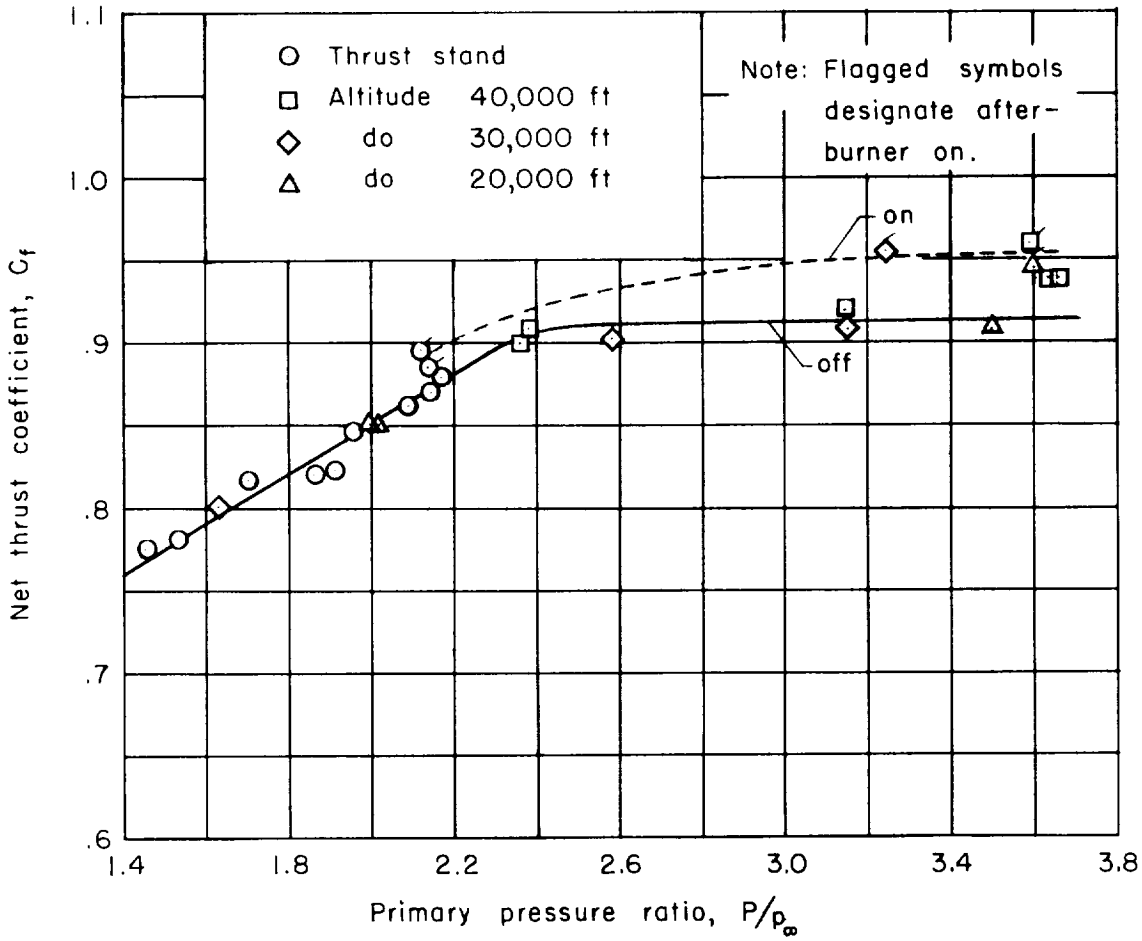

Figure 5.- Variation of the tail-pipe nozzle coefficient with primary pressure ratio as determined on a ground thrust stand and in flight.

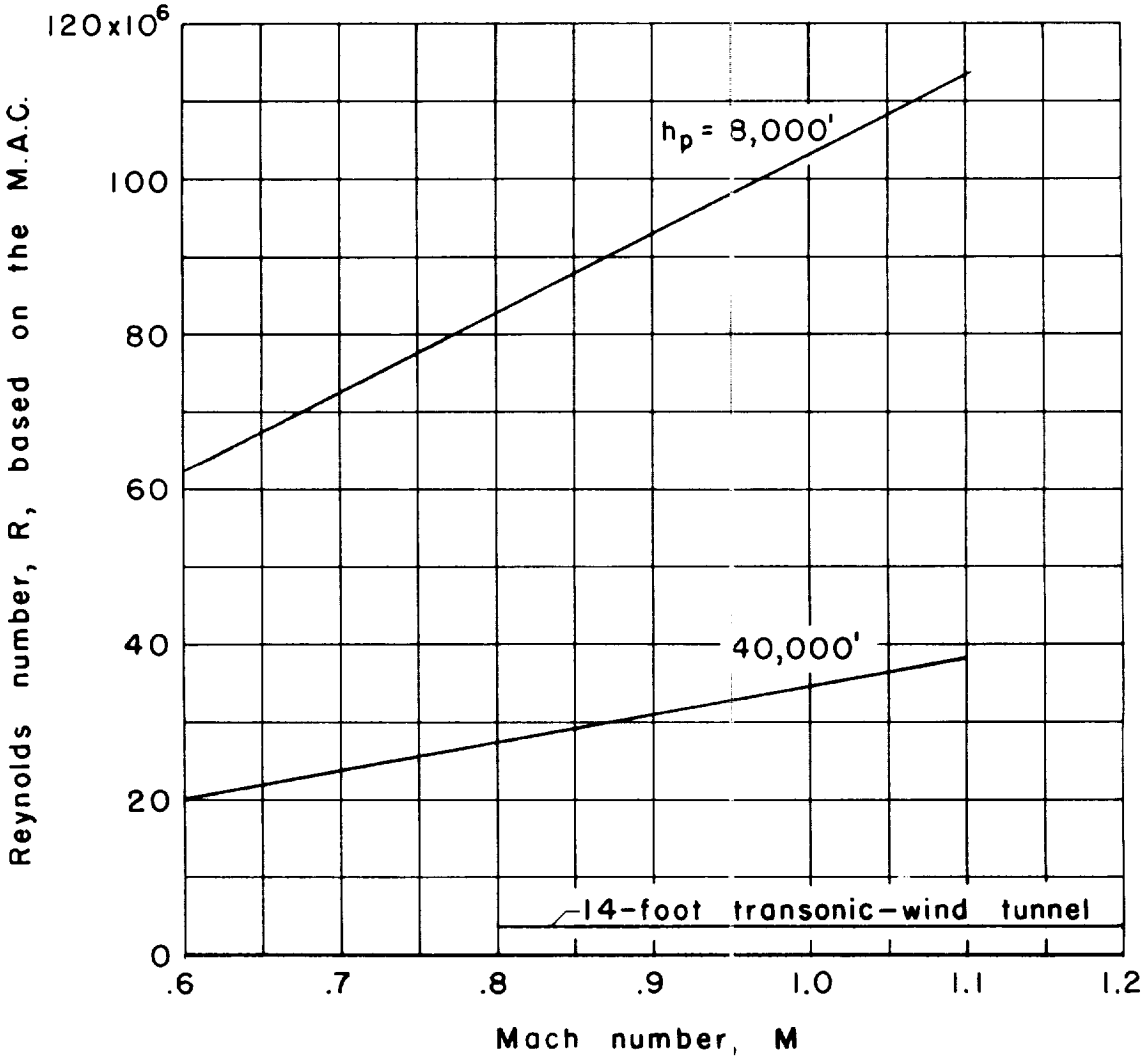

Figure 6.- Variation of Reynolds number with Mach number for the test conditions.

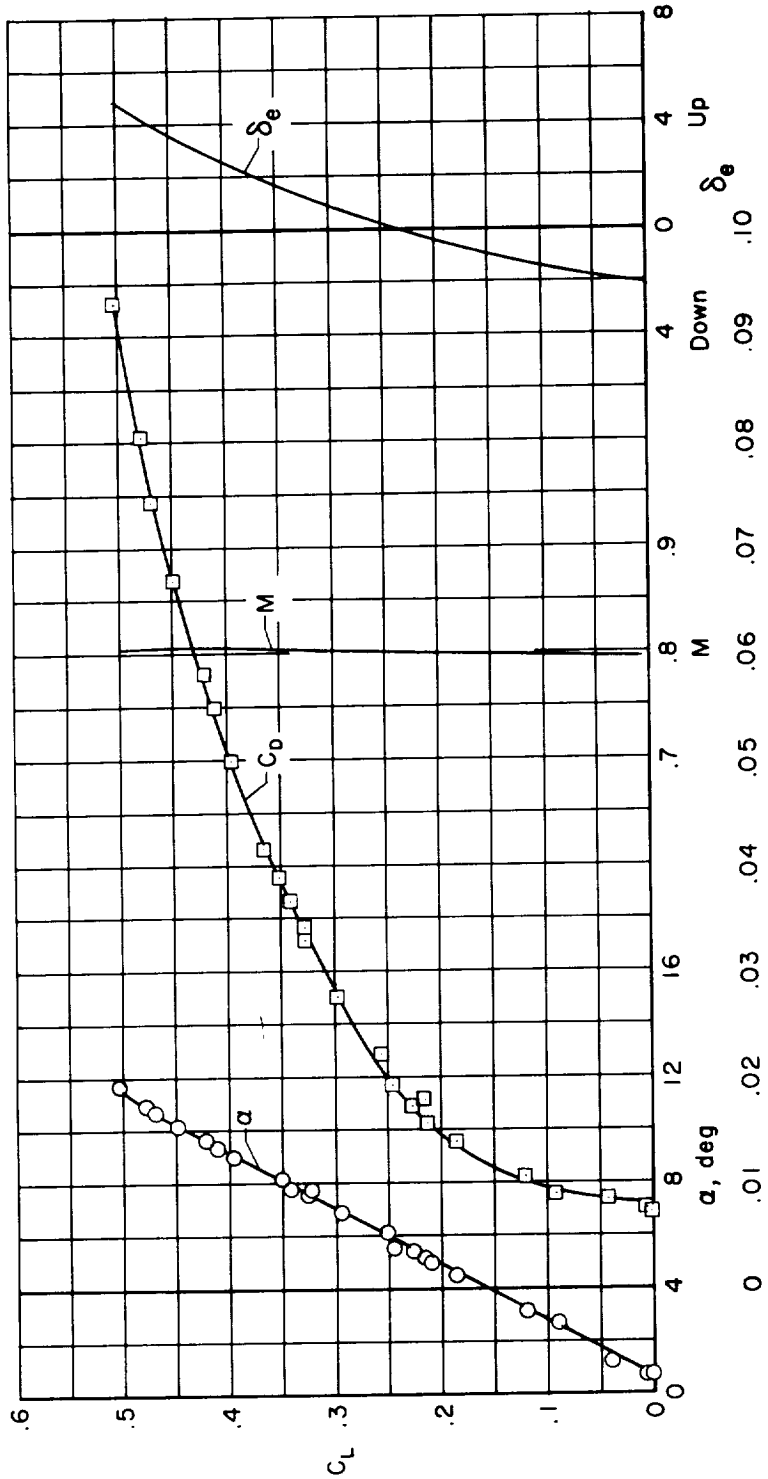

(a) M ≈ 0.80

Figure 7.- Variation of angle of attack, drag coefficient, and Mach number with lift coefficient during typical test maneuvers at an altitude of about 40,000 feet.

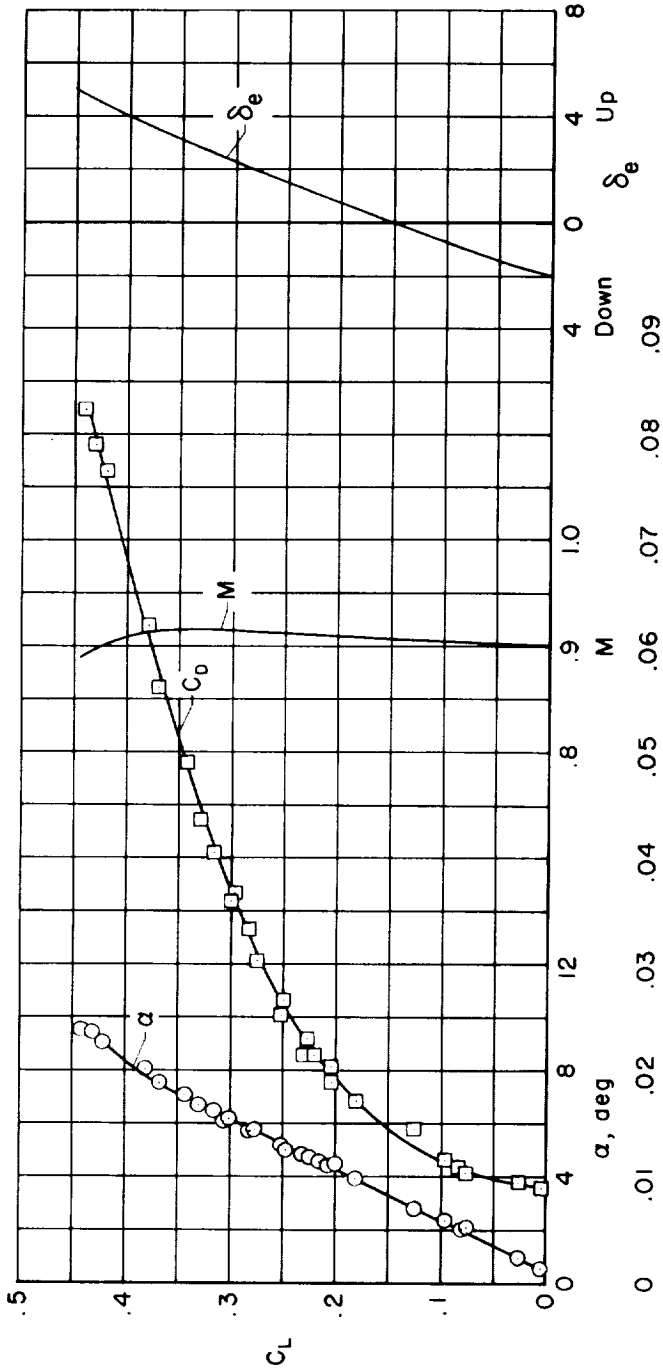

(b) M ≈ 0.90

Figure 7.- Continued.

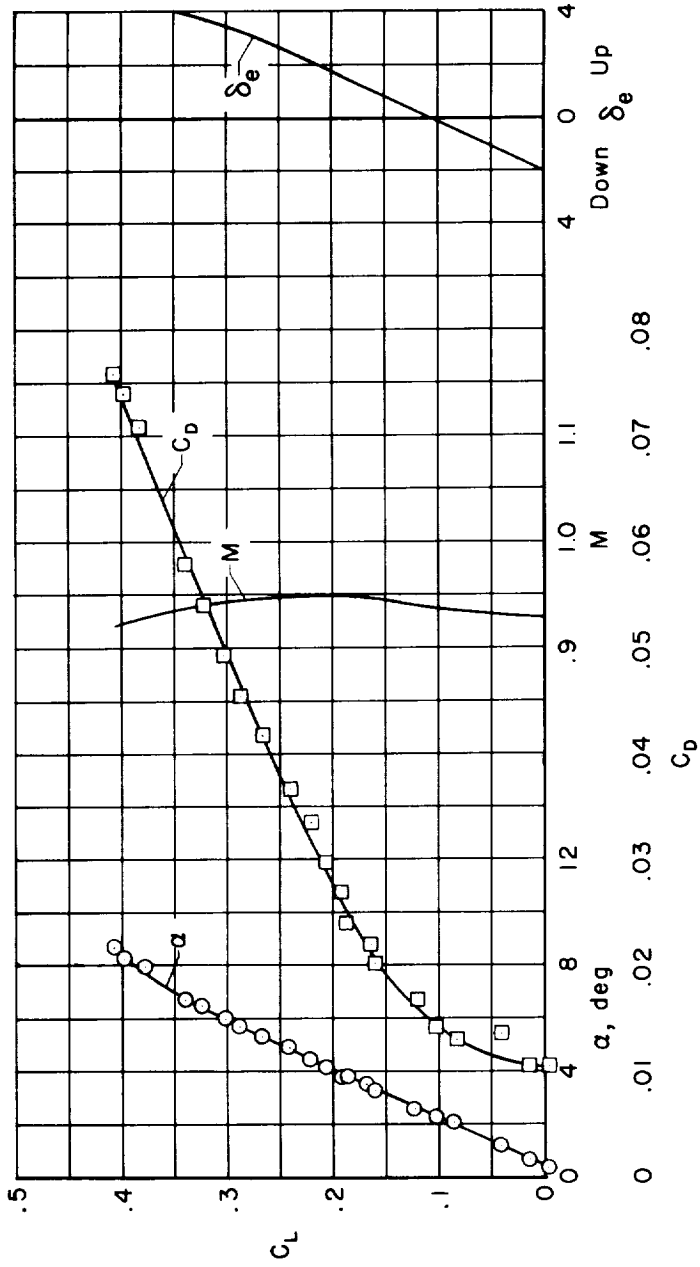

(c) M ≈ 0.93

Figure 7.- Continued.

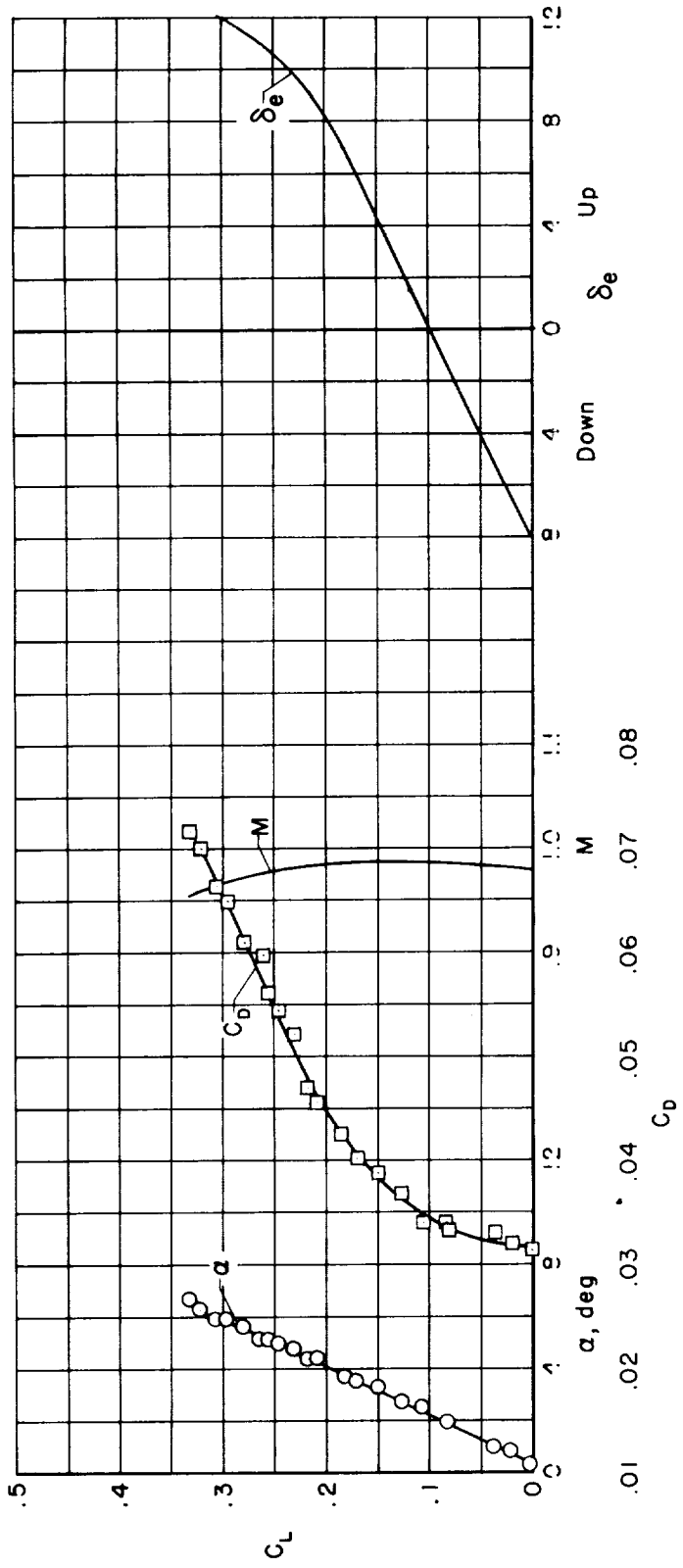

(d) M ≈ 0.98

Figure 7.- Continued.

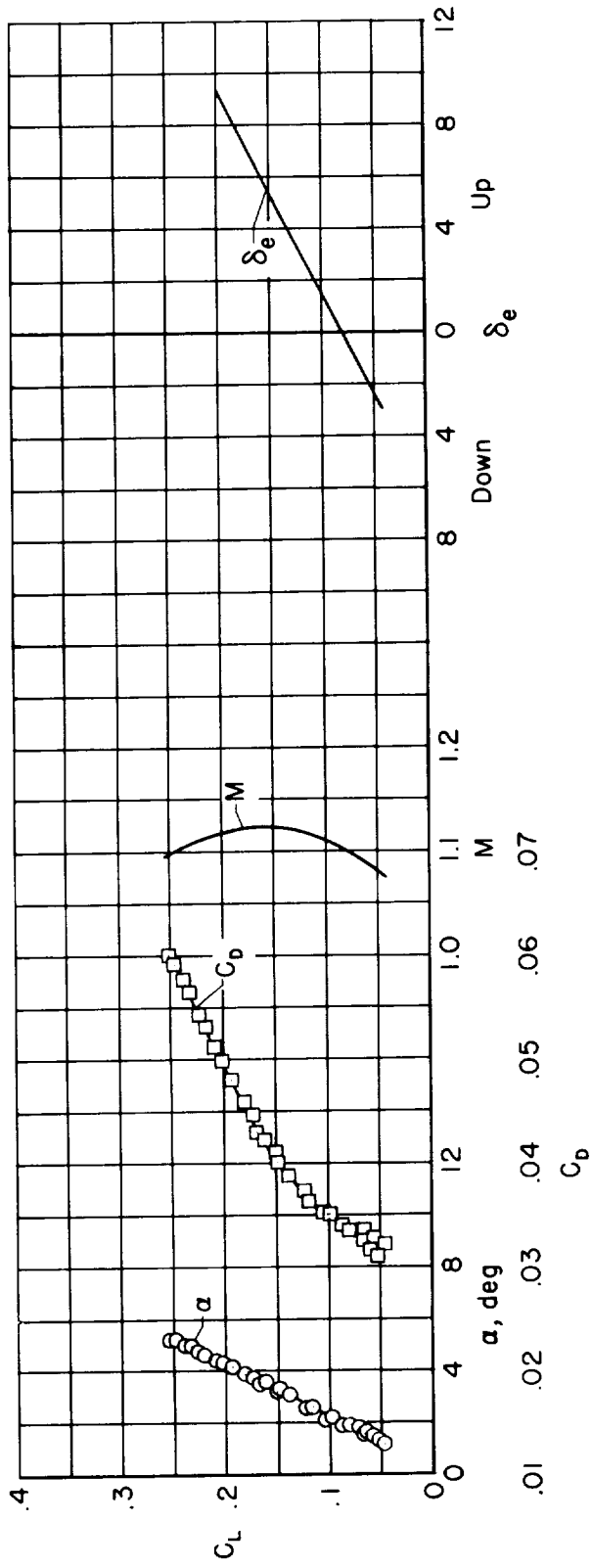

(e) M ≈ 1.10

Figure 7.- Concluded.

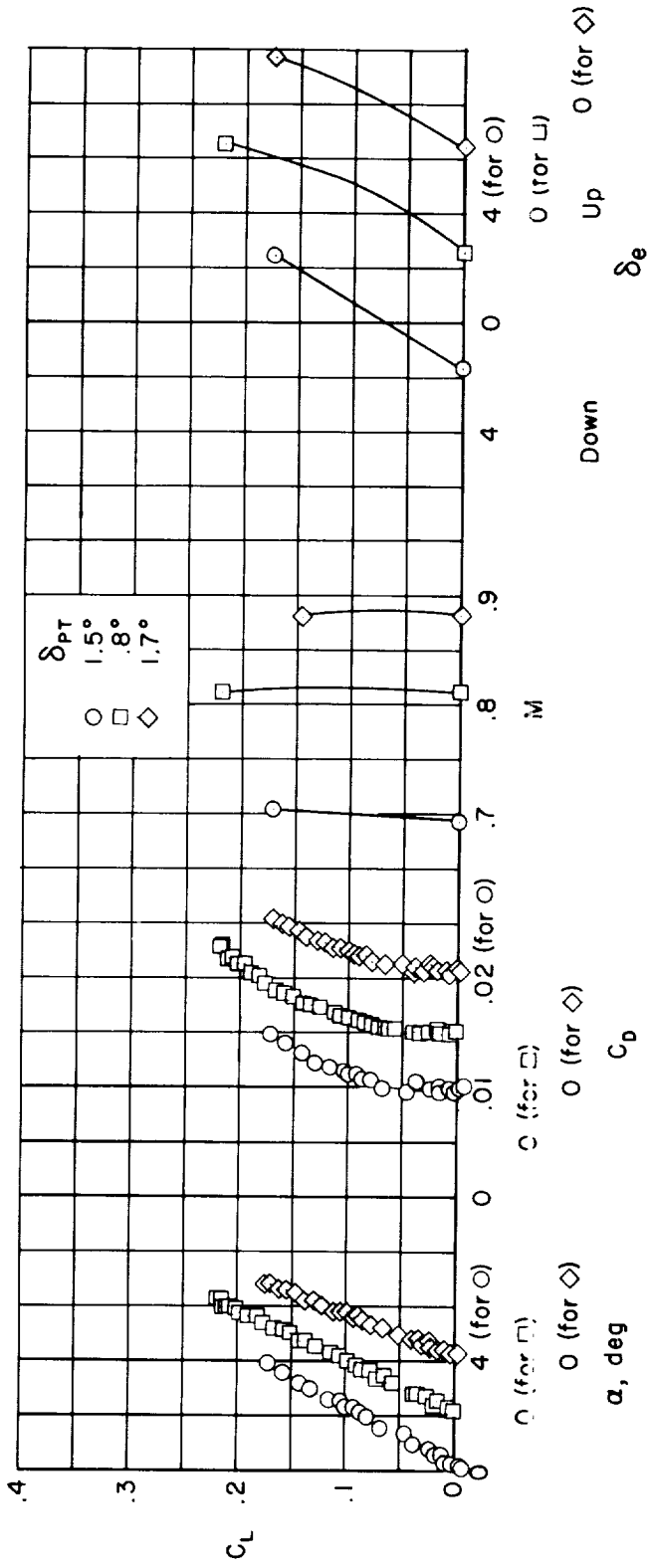

Figure 8.- Variation of angle of attack, drag coefficient, and Mach number with lift coefficient at a test altitude of 8,000 feet.

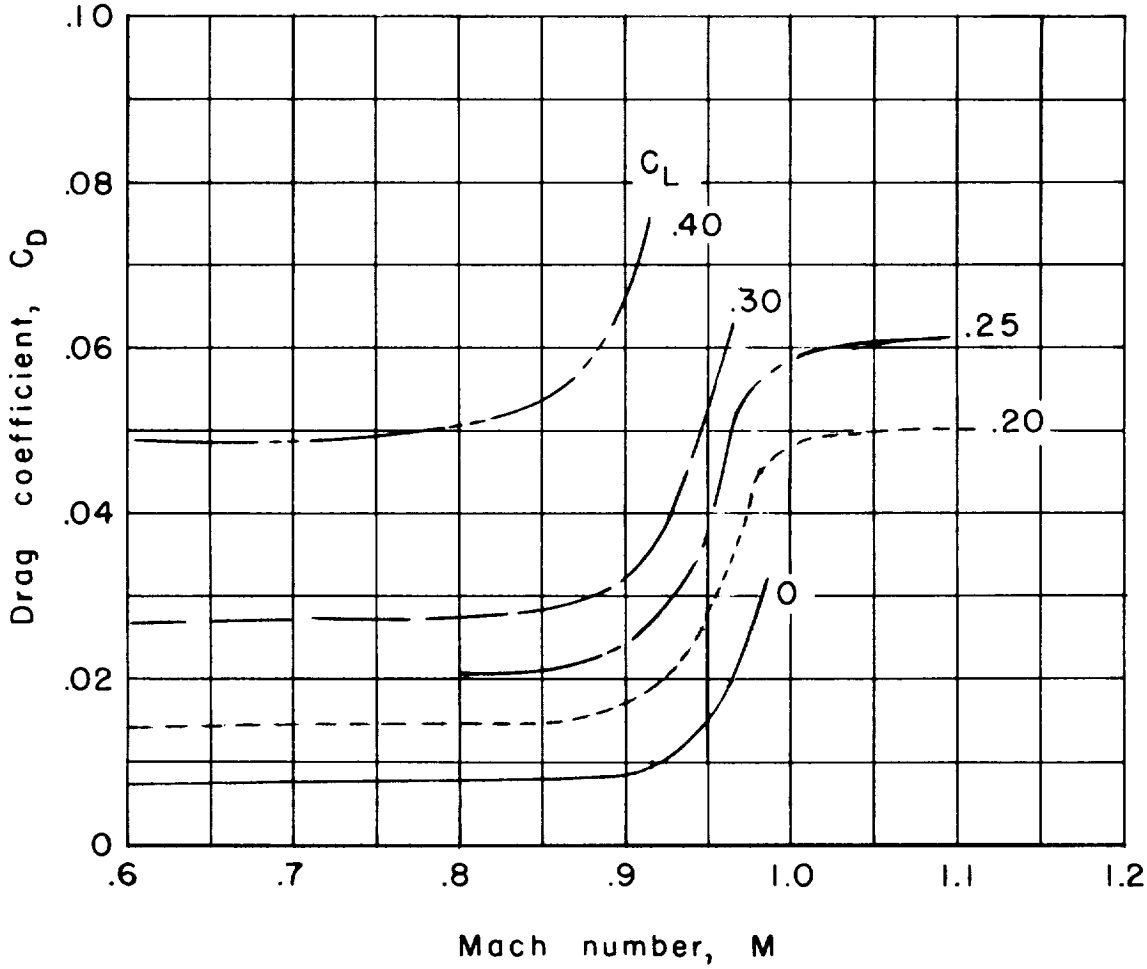

Figure 9.- Variation of trim drag coefficient with Mach number for several values of lift coefficient; altitude 40,000 feet.

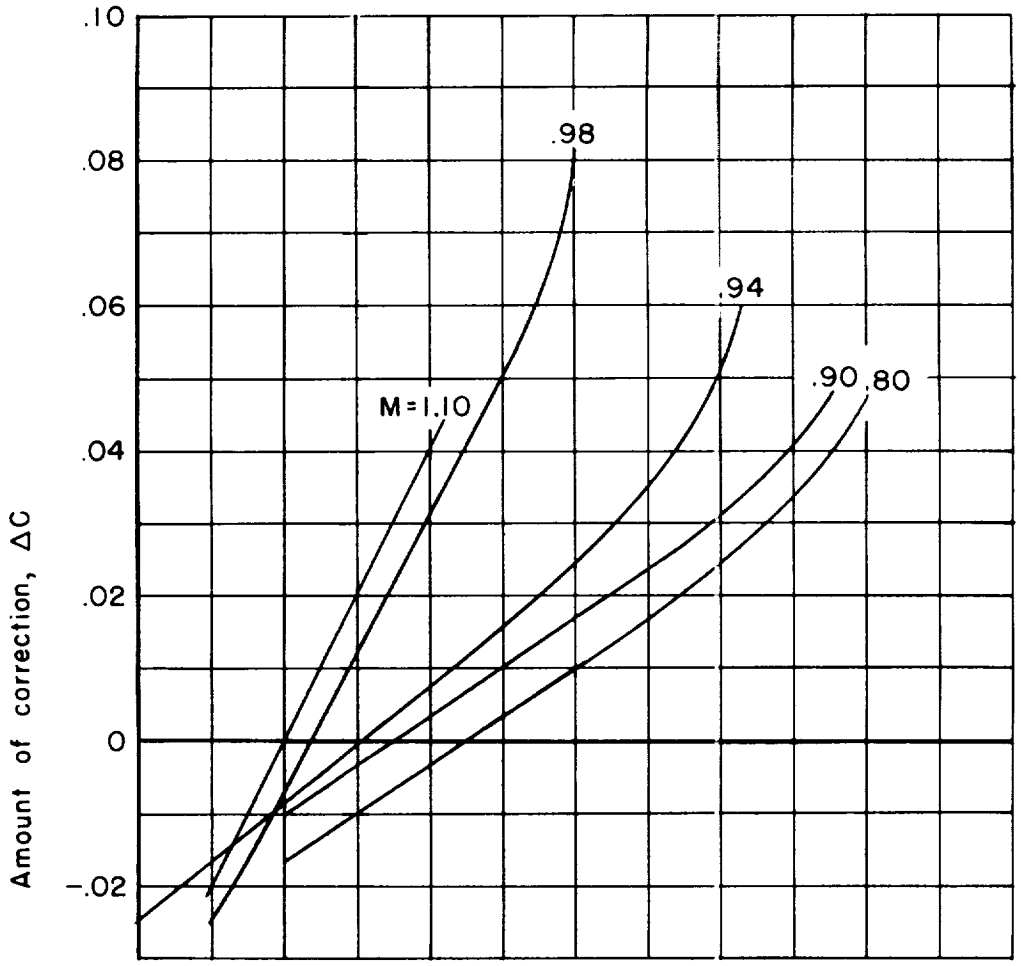

(a) Correction to lift coefficient.

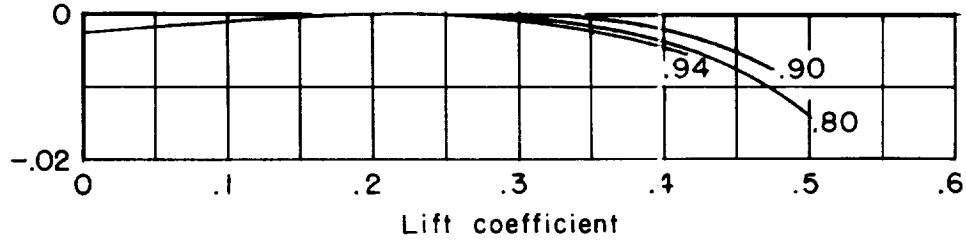

(b) Correction to drag coefficient.

Figure 10.- Correction applied to lift and drag coefficient due to elevon deflection.

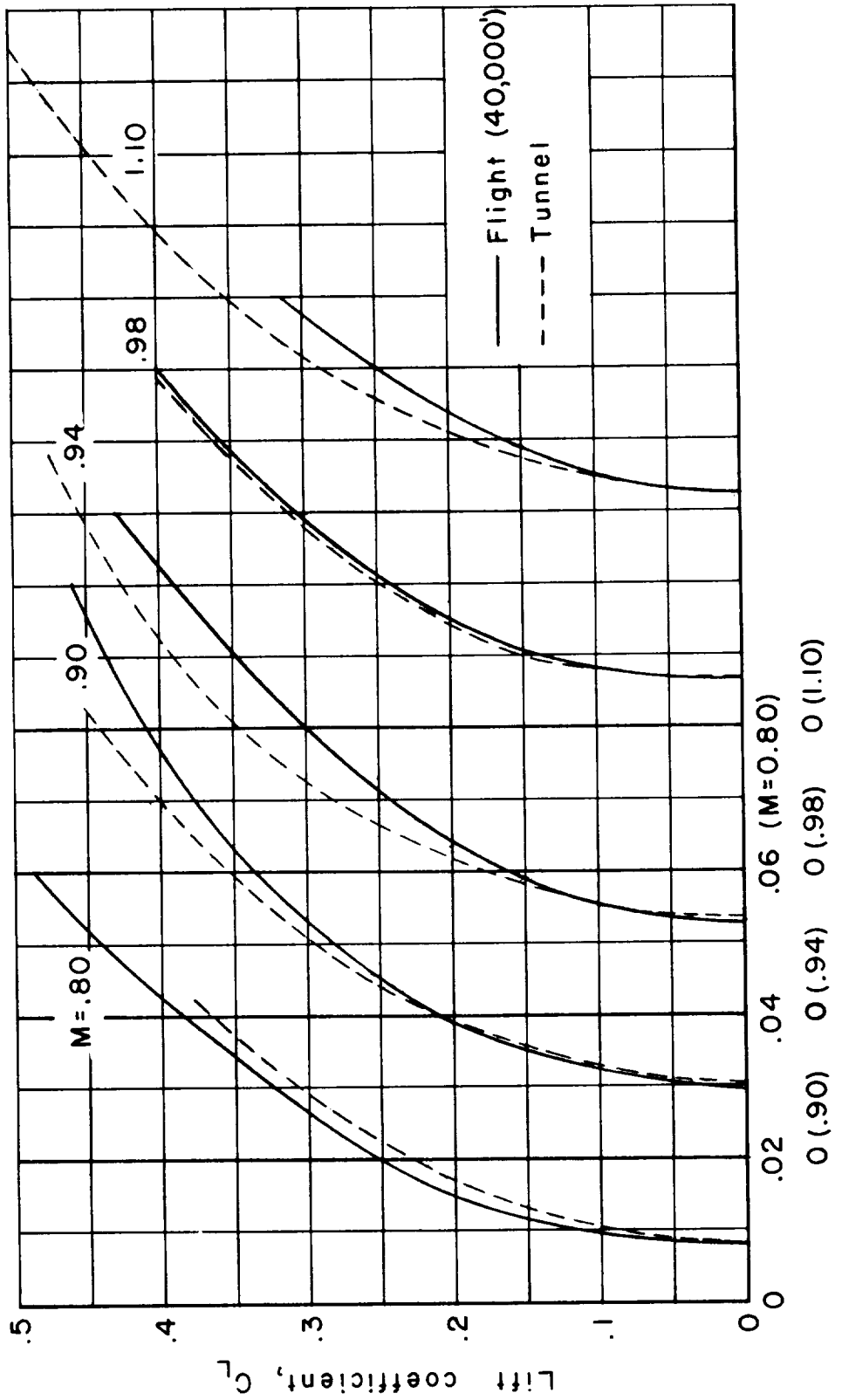

Figure 11. - Comparison of the drag polars measured in flight with those measured in the Ames 14-foot transonic wind tunnel; flight data corrected for elevon and trimmer deflection.

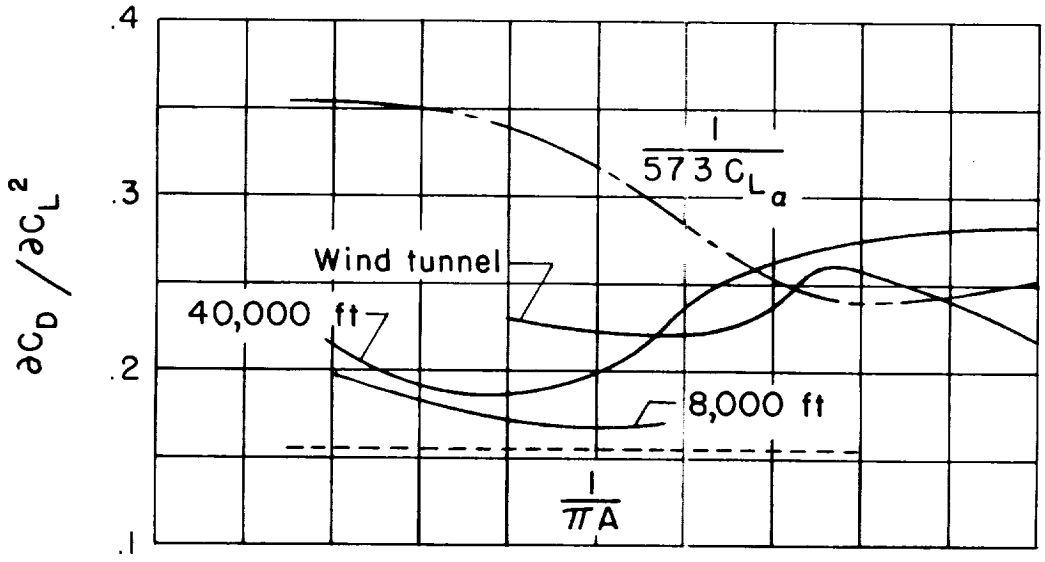

(a) Drag-rise factor.

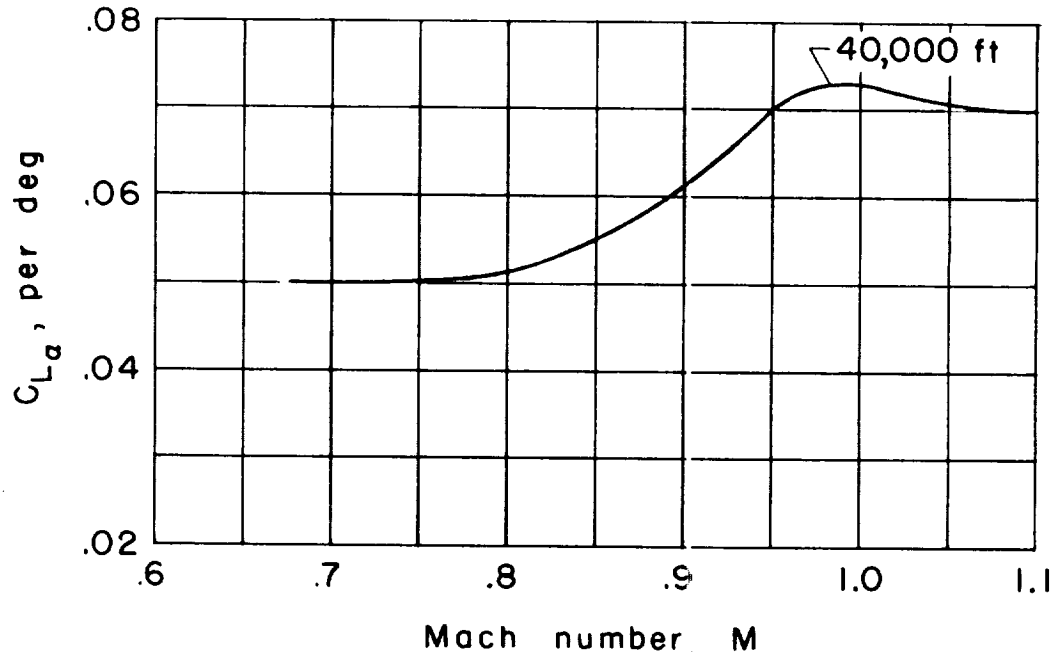

(b) Lift-curve slope.

Figure 12.- The variation of the flight and wind-tunnel measured drag due to lift and lift-curve slope with Mach number.

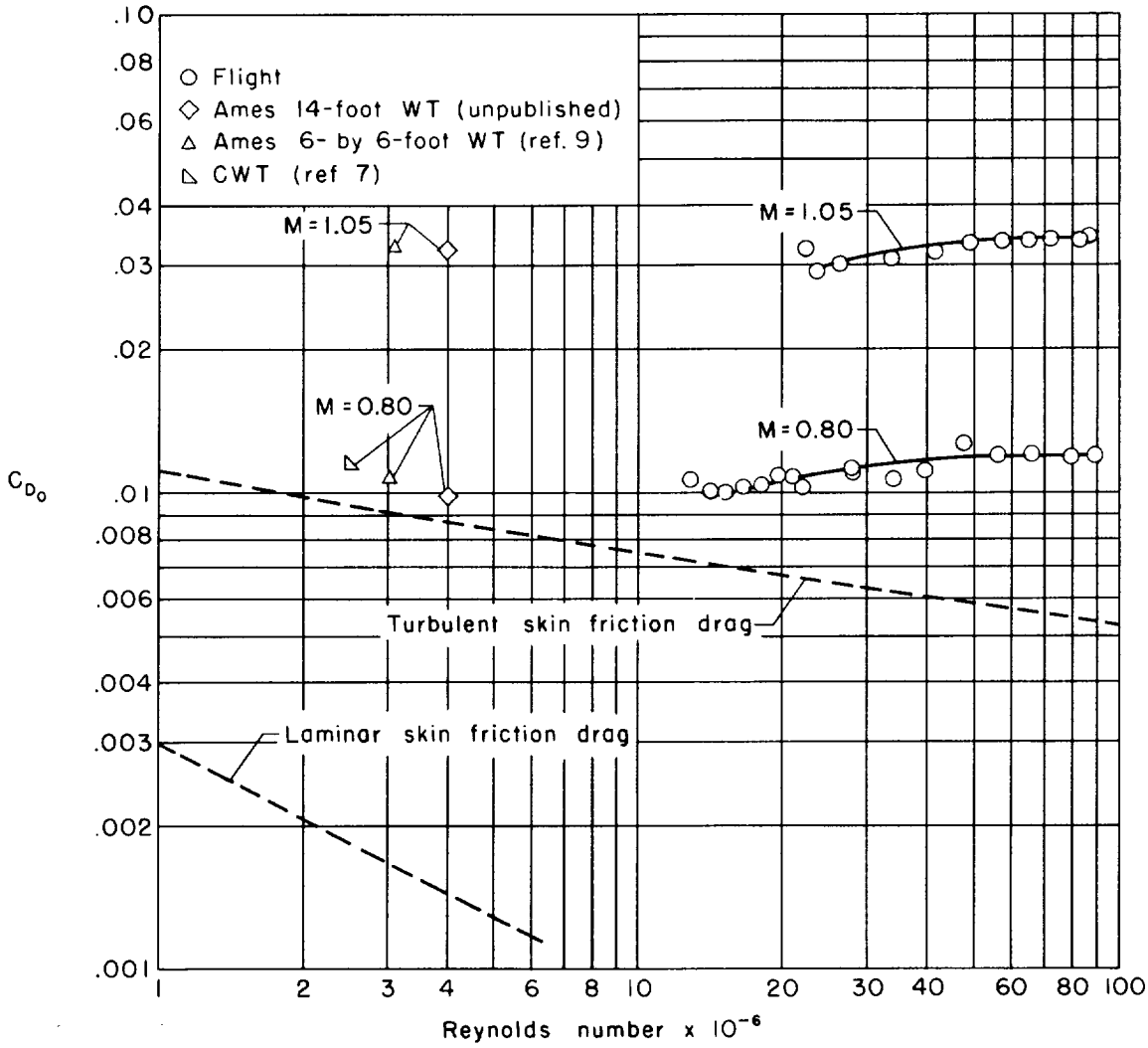

Figure 13.- Variation of C_{D_o} with Reynolds number for F4D-1 with $\delta_e = 0$.

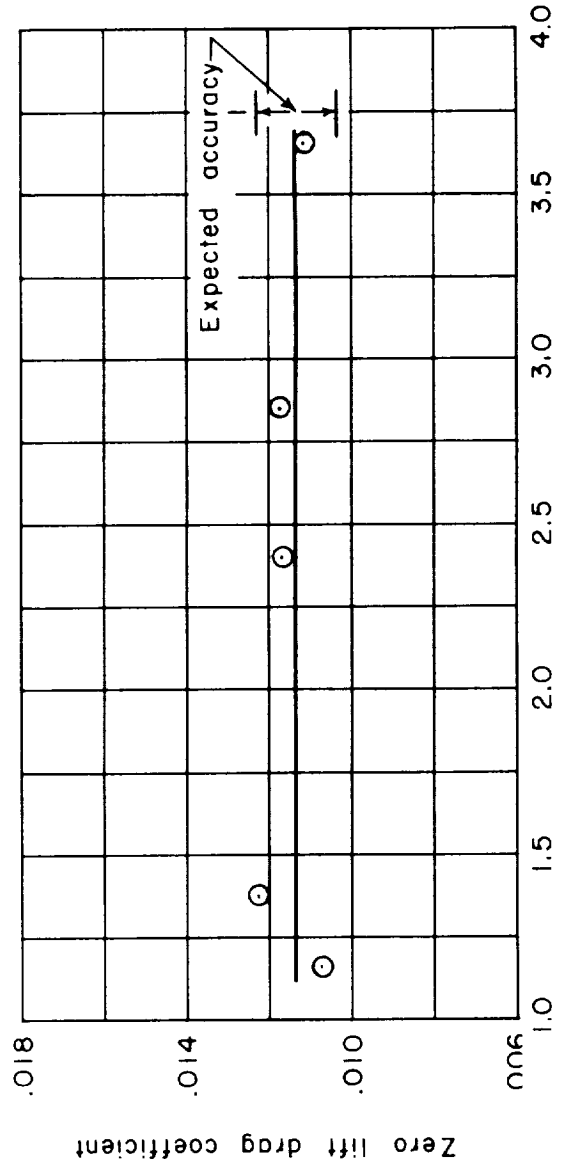

Figure 14.- Effect of changing engine power on the drag measured at a Reynolds number of 22 million; M = 0.80, h_p = 45,000 feet.

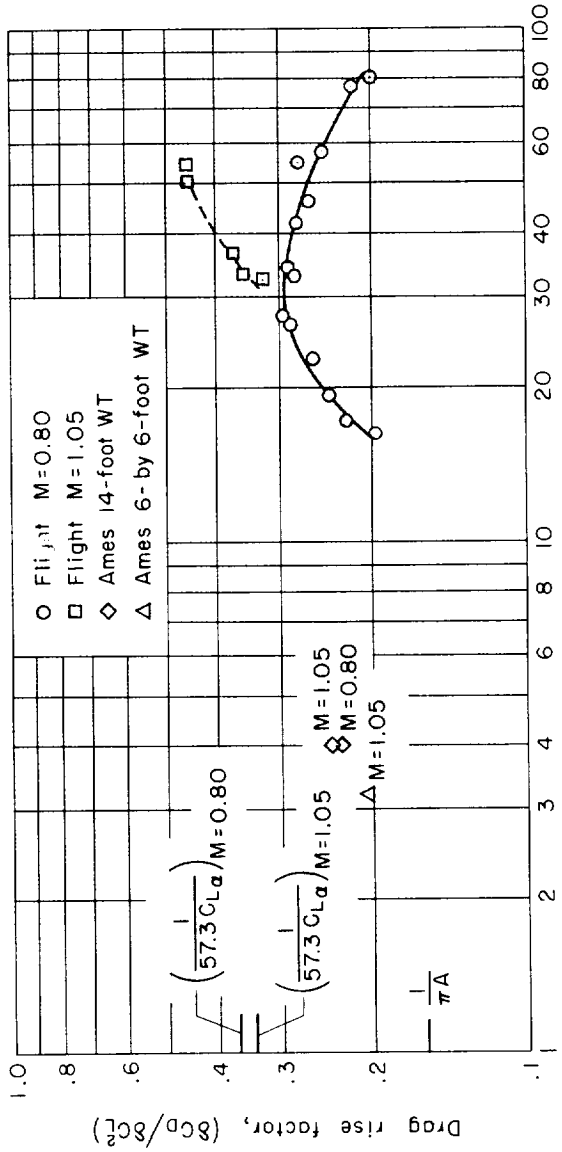

Figure 15.- Effect of Reynolds number on the drag due to lift; airplane trimmed.

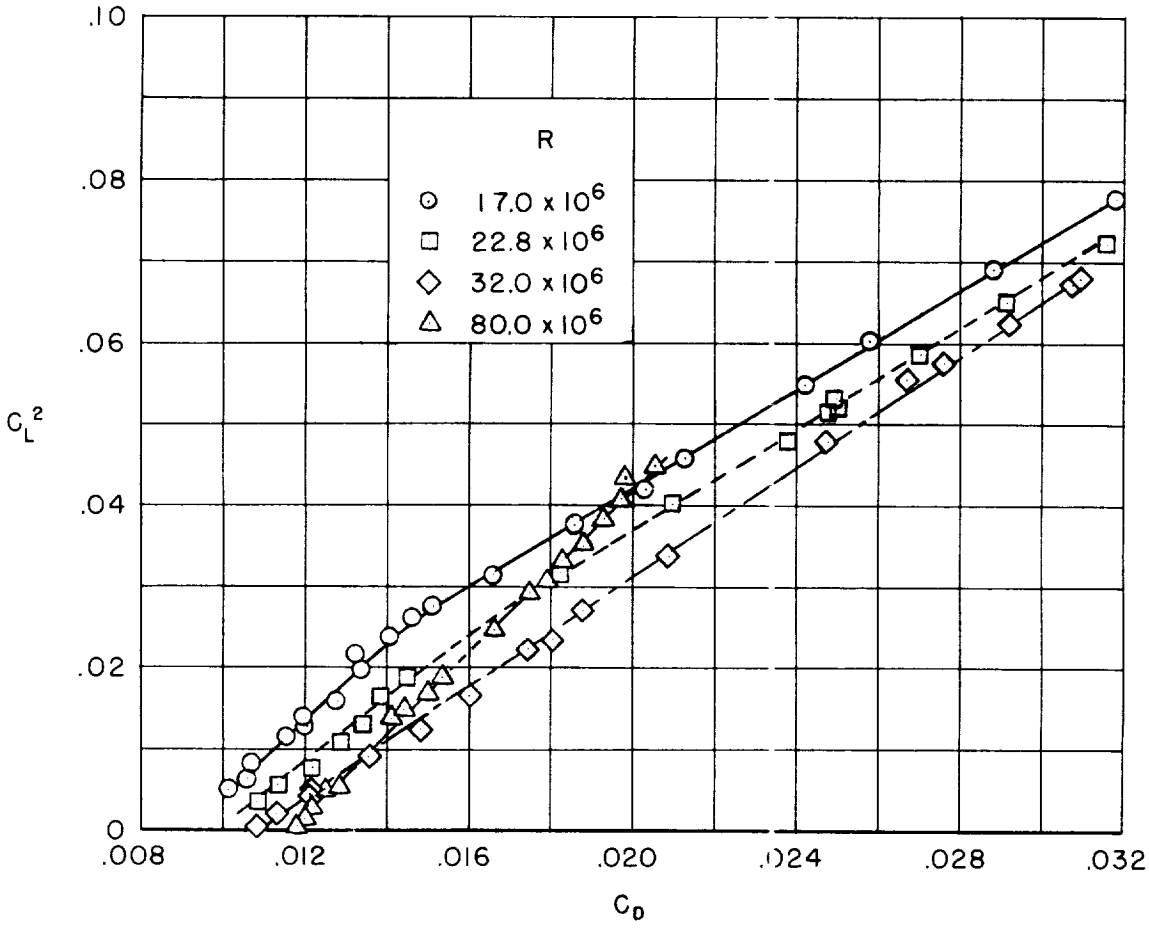

Figure 16.- The variation of drag coefficient with lift coefficient squared for different values of Reynolds number at a Mach number of 0.80.

NASA - Langley Field, Va.